RECONSTRUCTION OF THE HISTORY OF PACIFIC SARDINE AND NORTHERN ANCHOVY POPULATIONS OVER THE PAST TWO MILLENNIA FROM SEDIMENTS OF THE SANTA BARBARA BASIN, CALIFORNIA

TIM R. BAUMGARTNER[1]
División de Oceanología
Centro de Investigación Científica y de Educación Superior de Ensenada
Ensenada, Baja California, México

ANDY SOUTAR
Marine Life Research Group
Scripps Institution of Oceanography
University of California, San Diego
La Jolla, California 92093-0227

VICENTE FERREIRA-BARTRINA
División de Oceanología
Centro de Investigación Científica y de Educación Superior de Ensenada
Ensenada, Baja California, México

ABSTRACT

We present a composite time series of Pacific sardine and northern anchovy fish-scale-deposition rates developed from the anaerobic varved sediments of the Santa Barbara Basin off southern California. These series were constructed by integrating and adding to the data sets developed by Soutar and Isaacs and cover the period from A.D. 270 through 1970. We offer these series as a current best estimate of the sardine and anchovy scale-deposition rates and point out the sources and ranges of uncertainty remaining in the data. This includes providing a detailed analysis to determine the strength of the signal compared to the noise in scale-deposition rates.

We also recalibrate the scale-deposition data using available population estimates; we use this recalibration to hindcast the variability in sardine and anchovy stocks through almost 2000 years. Spectral analysis of the scale-deposition series shows that sardines and anchovies both tend to vary over a period of approximately 60 years. In addition, the anchovies fluctuate at a period of 100 years. The anchovy and sardine series show a moderate correlation over long time scales of several centuries or more; the correlation of shorter-period components in the time series is virtually nil. The scale-deposition record shows nine major recoveries and subsequent collapses of the sardine population over 1700 years. The average time for a recovery of the sardine is 30 years. A recovery is defined as an increase from less than one to over four million metric tons of biomass. We find that the current recovery is not unlike those of the past in its rate or magnitude.

RESUMEN

Presentamos series de tiempo de las tasas de depositación de escamas de la sardina del Pacífico y de la anchoveta norteña obtenidas de los sedimentos laminados anaeróbicos de la cuenca de Santa Barbara, al Sur de California. Estas series fueron construidas al integrar y completar los datos de Soutar e Isaacs e incluyen de 270 a 1970, D.C. Ofrecemos éstas series como la mejor estimación a la fecha de las tasas de depositación de escamas de sardinas y anchovetas y subrayamos las fuentes y rangos de incertidumbre quedando en los datos. Se incluye un análisis detallado para distinguir entre la fuerza de la señal respecto al ruido en las tasas de depositación de escamas.

También ofrecemos una recalibración de los datos de depositación utilizando estimaciones disponibles de la abundancia de la población. Utilizamos esta recalibración para estimar la variabilidad de los stocks de sardinas y anchovetas durante casi 2000 años. El cálculo del espectro de las series de depositación muestran que tanto las sardinas como las anchovetas tienden a variar con un periodo de aproximadamente 60 años, mientras que por otro lado las anchovetas fluctúan con periodo de 100 años. Las series de anchovetas y sardinas muestran una correlación mediana en escalas temporales de siglos o mayores, mientras que la correlación en periodos más cortos es virtualmente nula. El registro de depositación de escamas muestra que durante 1700 años la población de sardinas tuvo nueve recuperaciones principales seguidas de nueve colapsos. El tiempo promedio de recuperación de la sardina es de 30 años; se define recuperación como un incremento en la biomasa de menos de uno a más de cuatro millones de toneladas. Encontramos que el proceso de recuperación actual es similar a los del pasado en su tasa y magnitud.

INTRODUCTION

Traditional efforts to determine the fundamental time scales, and the sources, of variability in population sizes of Pacific sardine and other small pelagic fishes of the California Current are hindered because these stocks expand and contract over periods of several decades or longer. After roughly 60 years of annual biomass estimates for the Pacific sardine, fisheries scientists are able to describe only one major oscillation in its abundance. This oscillation appears to be nearing completion as the current sardine recovery gets well under way.

[1]Manuscript completed while a visiting scientist at the Marine Life Research Group, Scripps Institution of Oceanography, University of California, San Diego.

Fortunately, the annually layered (varved) sediments in the Santa Barbara Basin off southern California provide a natural historical record of pelagic fish populations (Soutar 1967). Not only does the Santa Barbara Basin underlie a portion of the spawning grounds of the Pacific sardine and northern anchovy, but also anaerobic conditions below sill depth preserve fish scales within a much more detailed chronological framework than is normal for marine sediments. Because they prevent the homogenization of sediments that results from mixing by benthic animals, anaerobic conditions produce a yearly memory of processes in the pelagic ecosystem.

Soutar and Isaacs (1969) developed time series of fish-scale counts for small pelagic species including the Pacific sardine and northern anchovy; these series were based on the analysis of a piston core from the Santa Barbara Basin and extend back over nearly two millennia. After developing these long time series, Soutar and Isaacs turned their attention to constructing shorter series covering the 160 years from 1810 through 1970. These series were based on a much expanded and therefore more reliable data base of four box cores (Soutar and Isaacs 1974). Development of these high-quality time series of scale-deposition data into the twentieth century also made it possible to compare and integrate the paleoecological record with direct estimates of population biomasses.

These data constituted the first continuous time series of fossil fish and offered a picture of variability over periods significantly greater than a century. Sequences of fossil scales have since been constructed from the slope sediments off Peru (DeVries and Pearcy 1982) and for the Benguela margin off West Africa (Shackleton 1986). But the lack of well-developed, continuously varved records in these places has so far prevented the reconstruction of time series to equal the quality of those from the Santa Barbara Basin. An overriding lesson from the Santa Barbara records is that in the past both sardines and anchovies experienced large natural fluctuations which were clearly unrelated to fishing, and that abrupt natural declines, similar to the collapse of the sardines during the 1940s, are not uncommon.

An obvious shortcoming in the study by Soutar and Isaacs (1969) is that the very small area sampled by a single piston corer (7.6-cm diameter) is used to represent scale deposition over the entire basin. Another constraint on their results derives from the uncertainty in the underlying chronology due to imperfect preservation of the annually deposited layers over the entire length of the record. One of the goals of this paper is to provide improved composite time series of sardine and anchovy scale deposition covering most of the past two millennia. We developed these new time series by integrating data from a second piston core with the original data presented by Soutar and Isaacs (1969), and by substituting the box core data for the upper portion of the two piston cores. The new sardine and anchovy series provide significantly more reliable estimates of the scale-deposition rates (SDR's) and are now presented as a continuous record from approximately A.D. 300 through 1970. The evolution of the improved SDR series is documented in the following section, along with a description of the efforts to achieve a more accurate chronological base for the series.

A second goal of this paper is to examine the quality and inherent limitations of the composite sardine and anchovy time series constructed by averaging information from the two piston cores. We have made a detailed analysis of the strength of the SDR signals relative to the noise that tends to obscure the information in which we are interested. This analysis is presented in the section "Signal-to-Noise Ratios in Scale-Deposition Rates," which documents the range of uncertainty in the SDR values and evaluates our current effort to provide reliable series for hindcasting the changes in fish populations. How the SDR series can be used to describe past variability in the sizes of sardine and anchovy stocks is illustrated in the section "Hindcasting Population Sizes from Scale-Deposition Rates."

Our final goal is to describe the principal time scales over which the variability occurs in the SDR series and to apply this information to a historical analysis of the inferred recoveries and collapses. This goal is met in the sections "Time Scales of Variability in the SDR Series" and "Recoveries and Collapses of the Pacific Sardine." We also compare past recoveries with the current one.

RECONSTRUCTING THE TIME SERIES OF SCALE-DEPOSITION RATES

The essential foundation for reconstructing any time series from the sediment record is the chronology assigned to a sediment column. Detailed radiometric dating of the modern laminated sediments in the Santa Barbara Basin with ^{210}Pb and $^{228}Th/^{232}Th$ has demonstrated that the light-dark lamina pairs are annually deposited varves (Koide et al. 1972; Soutar and Crill 1977; Bruland et al. 1981). Varved sediments began to form in the Santa Barbara Basin as early as 8000 years ago and have provided a much more detailed chronological framework for reconstructing paleoecologic and climatic histories than is

normally available from ocean basin and margin sediments (Soutar and Isaacs 1969; Soutar and Crill 1977; Heusser 1978; Pisias 1978).

The varve sequence of the anaerobic sediments of the Santa Barbara Basin is not continuous over the past 8000 years but is occasionally degraded by bioturbation and interrupted by turbidite deposition of centimeter-scale homogenous layers (Fleisher 1972; Soutar and Crill 1977; Schimmelmann et al. 1990). Although varve preservation for the past 2000 years is mostly good to excellent, episodes of bioturbation have disrupted the lamina sequence in varying degrees from negligible to complete erasure of the varve structure. These disturbances cover stratigraphic intervals of less than one to over many centimeters. Extending the annual chronology through these intervals (by interpolating sedimentation rates) leaves an inherent uncertainty proportional to the thickness of the interval, which accumulates downcore as more problem intervals are encountered. We now estimate the overall uncertainty to be approximately 50 years around the year 1000, which translates to roughly 5% over the length of the series. This estimate is based on comparisons of the SDR series to available high-resolution proxy records of climate change such as the tree rings of California bristlecone pines (LaMarche 1974). These comparisons suggest a possible chronological offset of 50 years near the midpoint of the series.

Soutar and Isaacs (1969) presented a time series (of continuous 10-year sample blocks) of fish-scale counts through the past 1800 years for the Pacific sardine, northern anchovy, Pacific hake, and a group of undifferentiated species including lampfish, saury, jack mackerel, and others. These series were developed from analyses of a 2.5-m core retrieved by a standard Kullenberg piston corer with 7.6-cm-diameter barrel. The location of this core is shown in figure 1 as core site 214 in the east-central basin area. Recently we combined results from the analysis of a second piston core from site 224 (figure 1) with the original series from site 214. Continuous records of the laminar varve structures in cores 214 and 224 were made by X-radiography of longitudinal slabs cut from the outside of the core. After identifying and matching the varve sequences from the radiographs of both cores, we assigned calendar dates to the varve record by counting from surface ages of box cores that correlated to the upper sections of the piston cores.

Cores 214 and 224 were continuously sampled at 1-cm intervals for wet sieving and separation of the

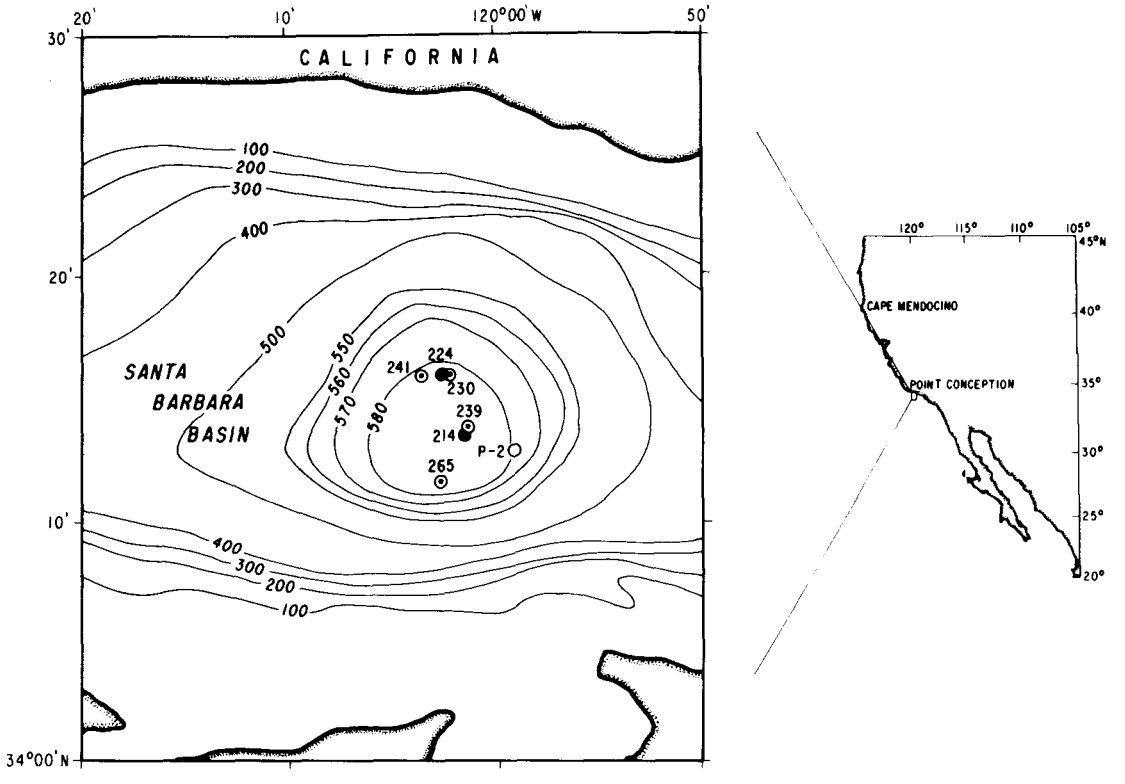

Figure 1. Locations of cores within the Santa Barbara Basin referred to in text. *Dark circles* are piston core sites (214 and 224) used to construct figures 2 and 3; *open circle* is piston core dated with tree-ring correlations (core P-2). *Circles with dots* are box cores (230,239,240,265) used to construct the short time series by Soutar and Isaacs (1974), which has been added to the series from the piston core sequence to obtain the series in figure 4.

fish debris (Soutar and Isaacs 1969). The time periods represented by the 1-cm subsamples range from 4 to 20 years, depending on the rate of sedimentation. Sampling based on depth downcore (the 1-cm slices) rather than on uniform varve (time) intervals results in only a slight loss of accuracy. The fish-scale counts with respect to depth were converted to scale-deposition rates over time (SDR's) by interpolation across the subsample thicknesses in order to adjust the values to 10-year intervals. To identify the scales we used a reference collection taken from fish caught off California and Baja California.

Figures 2 and 3 compare the time series reconstructed from cores 214 and 224 for the sardine and anchovy. It is important to note that the chronology used in these figures represents a preliminary stage of development, based solely on varve counts from X-radiographs and therefore subject to the necessary interpolation and bridging of poorly preserved and nonvarved intervals. Note also that the uppermost value plotted in figures 2 and 3 is from the interval 1800–1810. Because of the disturbance and loss of surface material associated with piston coring, it is prudent to disregard the uppermost section of the piston core. For a continuous record into the twentieth century, the period above 1810 is covered by the series developed by Soutar and Isaacs (1974) from the box cores at locations shown in figure 1.

Chronological uncertainty in varve sequences of the Santa Barbara Basin can be reduced by cross-correlating sequences of varve thicknesses to tree-ring widths because they are linked through rainfall in southern California (Soutar and Crill 1977; Schimmelmann et al. 1990). Cores 214 and 224 have not been directly dated by this method, but rather have been compared indirectly by correlation to a third piston core (P-2 in figure 1), for which the varve stratigraphy has been anchored with dates centered around 1405 and 770. Byrne et al. (in press) compare ring-widths of San Jacinto bigcone spruce (*Pseudotsuga macrocarpa*) from a 30-year interval (1391–1422) to the sequence of varve thicknesses to derive the best match from a lagged cross-correlation. The lower anchor point in core P-2 was obtained by cross-correlating the varve sequence to an 80-year tree-ring series (728–808) developed from *Pinus flexilis*. The *P. flexilis* series, however, is not as strongly correlated to varve thicknesses as are the *P. macrocarpa* series, and the lower anchor date is con-

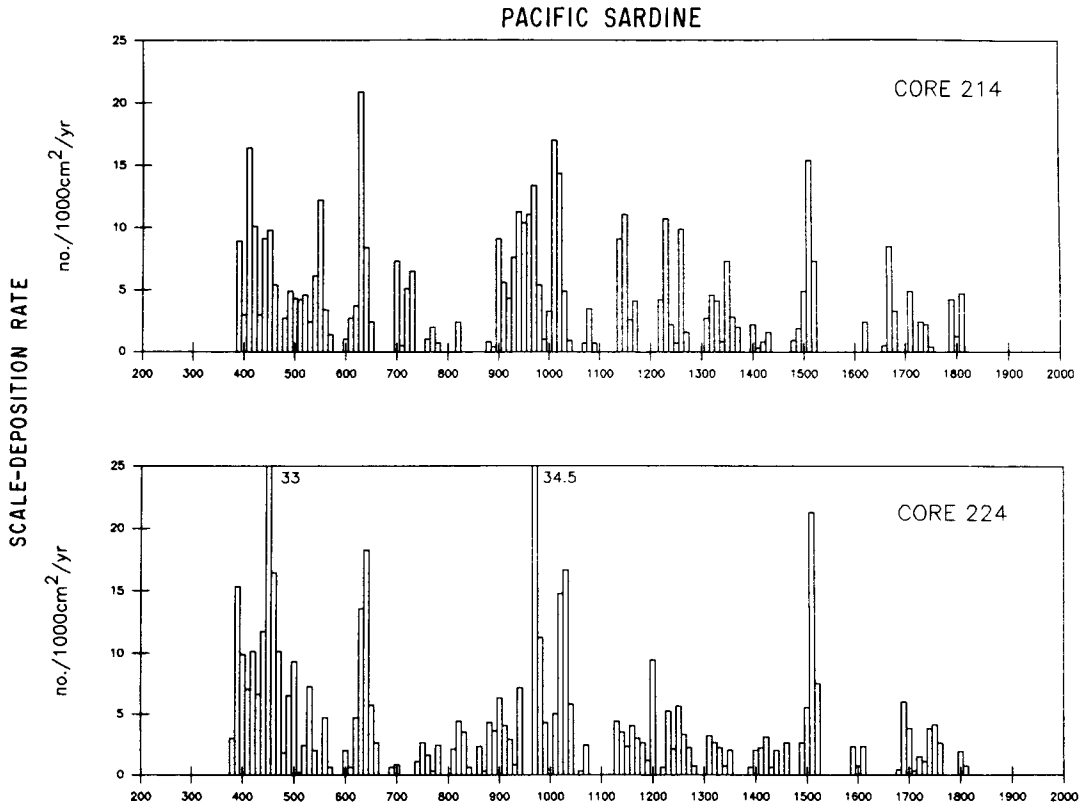

Figure 2. Original time series of scale-deposition rates for the Pacific sardine reconstructed at 10-year intervals from analysis of piston cores 214 and 224 from the Santa Barbara Basin (core sites in figure 1). The series is based on preliminary chronology; compare to figure 4. Scale-deposition rates are given as mean annual values for each 10-year period.

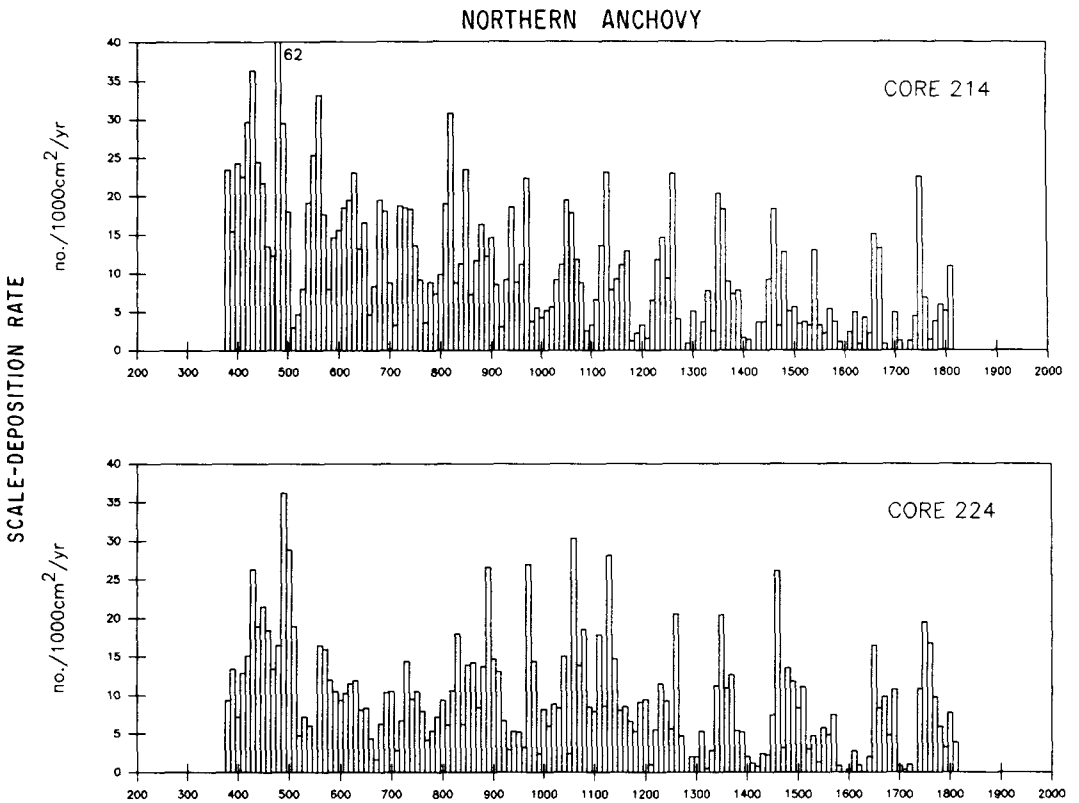

Figure 3. Original time series of scale-deposition rates for the northern anchovy reconstructed at 10-year intervals from analysis of piston cores 214 and 224 from the Santa Barbara Basin (core sites in figure 1). The series is based on preliminary chronology; compare to figure 4. Scale-deposition rates are given as mean annual values for each 10-year period.

sidered less reliable than the upper anchor date (J. Michaelsen, UC Santa Barbara, pers. comm.).

Figure 4 is a plot of the two composite time series of scale-deposition rates for the Pacific sardine and northern anchovy constructed by averaging the species SDR data from cores 214 and 224. Piston core P-2 (Byrne et al., in press) has been used as a chronological reference to adjust the original chronologies of cores 214 and 224 underlying the time series plotted in figures 2 and 3. The chronological adjustment to the fish-scale data in figure 4 was made by altering the calendar dates between the lower end of the series and the year 1100 in the original varve chronologies of figures 2 and 3. The chronology used for the interval 1100–1810 in the series of figure 4 is identical to that used in figures 2 and 3, whereas the lower end of the series in figure 4 is assigned an age 60 years younger than the original date. We completed this adjustment by compressing the data to fit into the decreased number of years by linear interpolation across the entire interval. This has a cumulative effect on the SDR values toward the lower end of the series as the chronological offset from the adjustment increases toward the maximum at the end of the record. When we take these adjustments into account, we can see the sardine and anchovy SDR series of figure 4 as the averages of the series in figures 2 and 3.

Values covering the period from 1810 through 1970 in figure 4 are based on the work published by Soutar and Isaacs (1974). These records were developed from four undisturbed, large-area (20 × 20 cm) box cores well distributed over the floor of the basin (figure 1; core sites 241, 230, 239, and 265). The chronology is very well constrained for the period of well-defined varve layering between 1860 and 1970, but less so for the period 1810–60, during which the sediments were subject to increased bioturbation, which somewhat degraded the laminar structure. Radiometric dating by ^{210}Pb and $^{228}Th/^{232}Th$ also provides a solid backup to the varve chronology above 1870. Scale-deposition rates were determined by sampling 5-year intervals down four longitudinal slabs (surface areas for each slab approximately 40 cm^2) from each of the four box cores.

Figure 5 shows the total area of depositional surface, plotted against calendar years, which has been sampled in the process of reconstructing the time series of scale-deposition rates in figure 4. The ex-

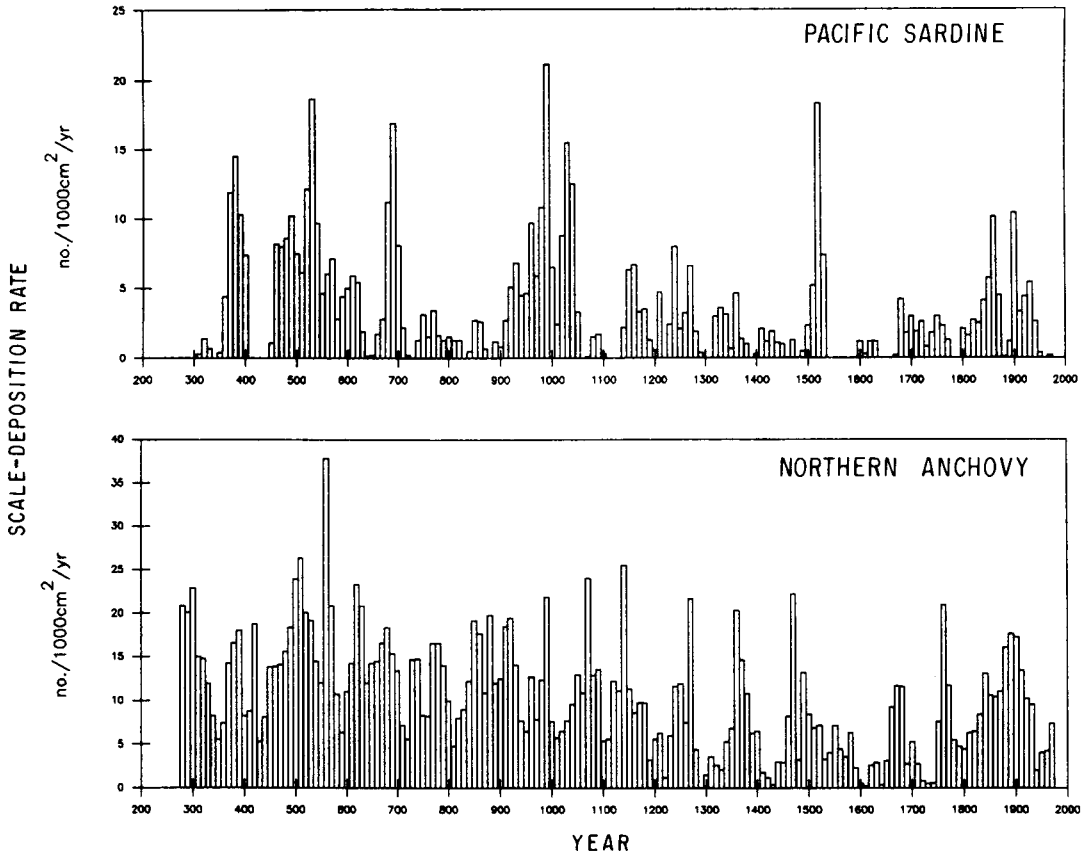

Figure 4. Composite time series of the Pacific sardine and northern anchovy scale-deposition rates developed by averaging across piston cores 214 and 224 (for the interval A.D. 270–1810; see figures 2 and 3) and by adding series developed from box cores 241, 230, 239, and 265 (for the interval 1810–1970). Note that the chronology used for these two time series is different (below A.D. 1100) from that of the original series in figures 2 and 3; it has been revised by correlation of varve chronostratigraphies from cores 214 and 224 to piston core P-2. Also note that 10 data points not plotted on figures 2 and 3 have been added to the beginning of figure 4.

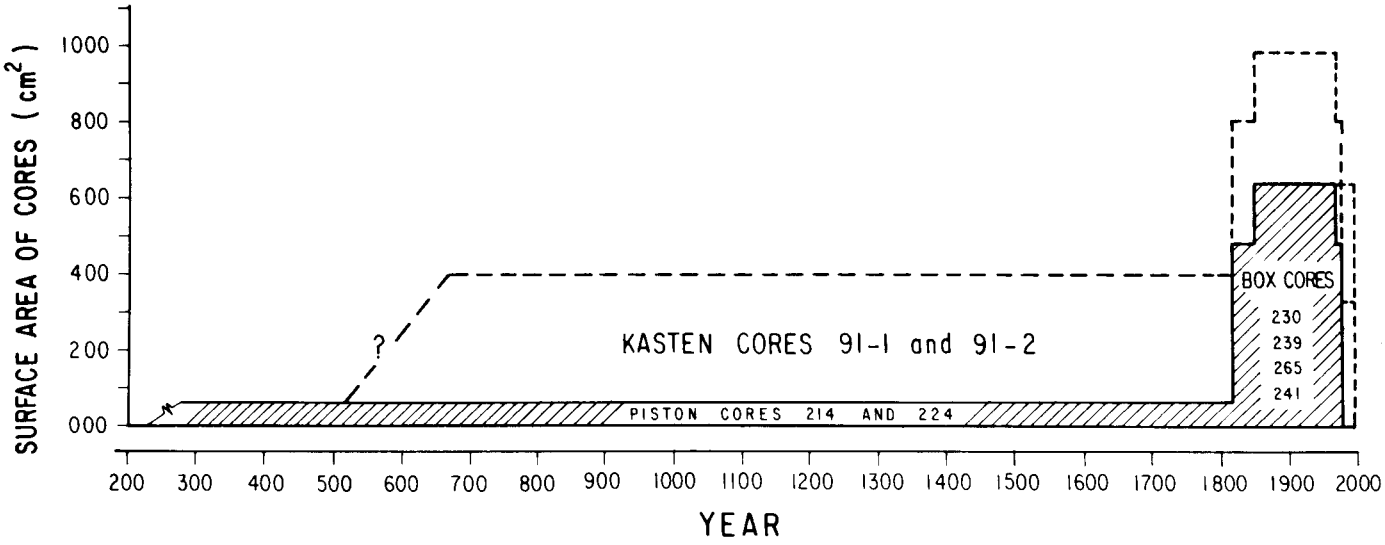

Figure 5. Diagram of the cumulative area of depositional surface sampled by the cores marked on location map in figure 1, plotted as a function of estimated calendar time sampled. *Hatched area* corresponds to the cores used to construct the sardine and anchovy SDR time series in figure 4. *Open area* represents the amount of material made available for future analysis by the recent recovery of two Kasten cores and two box cores from the Santa Barbara Basin.

panded data base for the period after 1810, obtained from the four box cores, should provide a much better averaged estimate of the SDR series than the data prior to 1810, which is based on the two small-diameter piston cores. We are now taking measures to expand this narrow data base. During 1991 we collected two high-quality Kasten cores, whose combined depositional surface areas are plotted in figure 5. These Kasten cores retrieved approximately 2.6 m of material and certainly reach at least 1500 years into the past.

Another important consideration bearing on the quality of the fish-scale numbers as a proxy record of populations is the extent to which diagenetic processes may have destroyed the buried scales. Evidence from both the stratigraphic distribution of scales and the interstitial water chemistry of the Santa Barbara Basin sediments indicate that degradation after deposition is negligible. Sholkovitz (1973) showed that the production of dissolved phosphate in the interstitial waters downcore is totally accounted for by decomposition of organic matter. This means that there is no "excess" phosphate present in the Santa Barbara Basin sediments to indicate dissolution of fish debris (as opposed to organically bound phosphorus) such as apparently does occur in sediments of the Peruvian margin (Suess 1981). The distribution of scales at depth also indicates that postburial degradation is not important, since there is no trend of decreasing scale numbers at depth for either sardines or anchovies in piston cores 214 and 224 (figures 2 and 3); on the contrary, there are clear tendencies toward increased SDR values downcore for both species in both cores.

SIGNAL-TO-NOISE RATIOS IN SCALE-DEPOSITION RATES

One of the most important questions regarding the use of fossil fish scales to hindcast population sizes addresses the reliability of the SDR values as indices of abundance. Part of this concern arises from our uncertainty about how well a single piston core represents the variability in scale deposition over the basin. A preliminary answer lies in comparing the time series of sardine and anchovy data from piston cores 214 and 224 plotted in figures 2 and 3. This comparison allows us to begin to characterize how well a "true" signal of the regional, or basin-wide, scale-deposition rate is visible above the noise induced either from sampling or from natural processes.

Note that this analysis does not specifically identify chronological error; rather we assume *a priori* a perfect "chronological" alignment among the time series analyzed. Therefore we must first obtain as good a match between the varve chronostratigraphies as possible. This produces a verifiable stratigraphic alignment between the two cores, but does not insure accurate agreement with calendar time. This is the case for the time series in figures 2 and 3. The varve stratigraphies matched one another, but the chronology by varve counting was subsequently modified below A.D. 1100 after comparison to core P-2. However, the chronological error does not alter the results of a signal-to-noise analysis, because the error is consistent in both cores.

The simplest means for an initial comparison are linear correlations among the sardine and anchovy data series from cores 214 and 224. The results of these correlations are given in table 1. We adjusted the significance levels of the correlation coefficients for the effects of autocorrelation within each of the series by calculating the reduced degrees of freedom for each correlation pair from the "integral time scales" as described in Enfield and Allen (1980). It is interesting that correlation between cores 214 and 224 for the sardines ($R = 0.53$) is the same as the between-core correlation for the anchovies ($R = 0.54$). These are respectable (and significant) correlations, although they indicate that the variance shared between cores for each species (R^2) does not exceed 30%.

Comparison of the above correlations with correlations between the two species in the same core and from different cores is also instructive: the correlation of the sardine series from core 214 with the anchovy series from 224 is virtually nil ($R = 0.16$; $R^2 = 0.03$), whereas correlation of the sardine series from core 224 and the anchovy series from the same core is significant, with a modestly high value of $R = 0.37$ ($R^2 = 0.14$). The fact that only about 30% of the variance is shared between series of the same species from the two cores indicates that the data in figures 2 and 3 must contain a substantial quantity

TABLE 1

Correlation Matrix of the Time Series of Pacific Sardine and Northern Anchovy from Cores 214 and 224

	Anchovy 214	Anchovy 224	Sardine 214	Sardine 224
Anchovy 214		0.54	0.26	0.24
Anchovy 224	(65) .001		0.16	0.37
Sardine 214	(80) .05	(92) .20		0.53
Sardine 224	(77) .05	(92) .001	(95) .001	

Note: Correlation coefficients (R) are shown above the diagonal. Levels of significance (α) and the reduced degrees of freedom (shown in parentheses) obtained from the "integral time scales" of the correlation pairs (see text) are given below the diagonal. Length of all series is $N = 144$.

of uncorrelated noise. Conversely, the shared signals are clearly detectable by the correlations.

Determining the actual ratio of the signal to noise in the SDR data of figures 2 and 3 can be approached by a two-way analysis of variance performed separately for the sardine and anchovy SDR series of the two piston cores in order to distinguish among the different sources of variability. Comparison of the sardine or anchovy SDR series from the two cores follows an experimental design (Griffiths 1967; chap. 19) in which each observation $x_{i,j}$ can be expressed by the linear model

$$x_{i,j} = \mu + \alpha_i + \beta_j + \epsilon_{i,j}$$

indicating that any observation of the two series comprises an estimate of the overall mean value μ, plus a contribution from the effect of downcore variability α_i (this is the time-dependent *signal* in which we are interested), plus a contribution from the effect of β_j associated with the difference between the j core sites (a consistent difference through time in deposition of fish scales from one site to the next), plus a contribution from random "errors", ϵ_{ij} (the undifferentiated between-core and downcore *noise*), occurring among the i samples down each core. Note that this design assumes there is no "interaction" (dependence) between the downcore, temporal variability and the between-core, spatial variability (i.e., $\alpha\beta_{ij} = 0$). This assumption is necessary because we lack the replicate subsamples within each core to estimate any effect from $\alpha\beta_{ij}$ (Griffiths 1967; chap. 19).

Table 2 displays the results of the two-way ANOVA for the sardine data; the same information for the anchovy data is given in table 3. These tables

TABLE 2

Results of the Two-Way Analysis of Variance on the Sardine SDR Series from Cores 214 and 224 Plotted in Figure 2

No. of items	Source of variation	d.f.	Sum of squares	Mean square
a = 144	Downcore signal	143	5221.372	36.5103 $(b\sigma_\alpha^2 + \sigma_\epsilon^2)$
b = 2	Between-core effect	1	6.037812	6.03781 $(a\sigma_\beta^2 + \sigma_\epsilon^2)$
	Noise	143	1692.447	11.8353 (σ_ϵ^2)
ab = 288	Total	287	6919.857	

Ratios of mean square value of the downcore signal and the between-core effect to the mean square value of noise	Observed F				Test statistic F_{os}
Downcore signal : noise (143 d.f. : 143 d.f.)	$\frac{36.51}{11.84}$	=	3.08	>	1.32
Between-core effect : noise (1 d.f. : 143 d.f.)	$\frac{6.04}{11.84}$	=	0.51	<	3.91

TABLE 3

Results of the Two-Way Analysis of Variance on the Anchovy SDR Series from Cores 214 and 224 Plotted in Figure 3

No. of items	Source of variation	d.f.	Sum of squares	Mean square
a = 144	Downcore signal	143	14512.07	101.4830 $(b\sigma_\alpha^2 + \sigma_\epsilon^2)$
b = 2	Between-core effect	1	140.4209	140.4209 $(a\sigma_\beta^2 + \sigma_\epsilon^2)$
	Noise	143	4558.724	31.8792 (σ_ϵ^2)
ab = 288	Total	287	19211.21	

Ratios of mean square value of the downcore signal and the between-core effect to the mean square value of noise	Observed F				Test statistic F_{os}
Downcore signal : noise (143 d.f. : 143 d.f.)	$\frac{101.48}{31.88}$	=	3.18	>	1.32
Between-core effect : noise (1 d.f. : 143 d.f.)	$\frac{140.42}{31.88}$	=	4.40	>	3.91

show the partitioning of the total variance by the analysis into the mean square values associated with three sources of variability: the downcore, temporal signal ($b\sigma_\alpha^2 + \sigma_\epsilon^2$); the constant between-core difference ($a\sigma_\beta^2 + \sigma_\epsilon^2$); and the unexplained noise (σ_ϵ^2).

The significance of contributions from the downcore signal and the between-core difference versus the unassigned noise is found by comparing their respective mean square values through a variance ratio F test (Griffiths 1967; chap. 19). Using the F statistic we can test the hypotheses

(1) H_o: The variance of the noise is equivalent to the downcore signal ($\sigma_\alpha^2 = \sigma_\epsilon^2$), against

H_a: The variance of the downcore signal is significantly greater than that of the noise ($\sigma_\alpha^2 > \sigma_\epsilon^2$)

and

(2) H_o: The variance of the noise is equivalent to the between-core effect ($\sigma_\beta^2 = \sigma_\epsilon^2$), against

H_a: The variance of the between-core effect is significantly greater than that of the noise ($\sigma_\beta^2 > \sigma_\epsilon^2$).

Table 2 shows that for the sardine data the first null hypothesis above can be rejected; the observed value of F (3.08) is greater than the tabulated value (1.32) at the 95% level of confidence. Therefore, the ANOVA does clearly distinguish between the downcore signal and the undifferentiated noise. The mean square value of the signal is threefold that of the noise. This is substantially more than is needed to reject the first null hypothesis.

Table 2 further shows that the second null hypothesis above cannot be rejected; the observed value of F (0.51) is considerably less than the tabulated value (3.91) at the 95% level. This means that the ANOVA cannot detect a between-core effect above the noise. There appears to be no significant consistent difference in deposition of sardine scales between cores 214 and 224.

Table 3 shows that both null hypotheses are rejected in the analysis of the anchovy series. Therefore, the ANOVA does also clearly distinguish a regional downcore signal above the residual temporal-spatial noise in the anchovy data. Like the downcore sardine signal, the anchovy signal is three times that of the noise. However, in contrast to the sardine ANOVA, we find here a measurable difference in anchovy scale deposition between cores 214 and 224. Although this suggests some pattern of nonuniform deposition of anchovy scales within the basin, we cannot determine the spatial scale of this suggested variability (is it basinwide or does it occur, for example, over small distances of centimeters to meters?) or distinguish any temporal-spatial interaction. This result stresses the need for multiple-site sampling within the basin using coring devices that retrieve surface areas large enough to allow for replicate determinations within each core (cf. figure 5).

HINDCASTING POPULATION SIZES FROM SCALE-DEPOSITION RATES

Another major concern over the value of SDR's for estimating population sizes is how sensitive the "true" basin-wide SDR signal is to changes in regional abundance (density) of fish. One of the major accomplishments by Soutar and Isaacs (1974) was to demonstrate that the rates of fish-scale deposition in the Santa Barbara Basin provide reasonable indices to changes in the population biomasses, particularly for sardines and anchovies in the California Current. Their comparison of SDR's to biomass was based on a 5-year sample resolution obtained from the analysis of the box cores.

Soutar and Isaacs (1974) were able to establish a relationship between SDR values and the six 5-year averages of available annual estimates of the total sardine population from 1932 to 1960 obtained by Murphy (1966). They also found an exceptionally good relationship between sardine SDR and the biomass of fish younger than 2 years old, consistent with the observation that most of the scales (greater than 90%) found in the sediments were from fish less than 2 years old. This indicates that scale deposition is sensitive to the density of fish in the immediately overlying water column. The relationship between the scales and the biomass of the 2-year-old and older fish was diminished but still clearly significant, and demonstrated that the Santa Barbara SDR's are also proportional to the adult biomass off California and northern Baja California. Thus the response of the SDR's to the larger population biomass appears to occur through an indirect relationship between the numbers of younger fish inhabiting the area inshore over the Santa Barbara Basin and the total adult populations over their respective ranges.

It is now possible to recalibrate the sardine SDR data to biomass estimates by using revised population estimates for the years 1945–65 presented by MacCall (1979), coupled with Murphy's (1966) esti-

mates for 1932–44, and by assuming that the population had shrunk to under 20,000 metric tons (MT) after 1964. This provides an improved series of biomass estimates, and we gain two more data points than were available to Soutar and Isaacs (1974) for the sardine SDR's. The upper diagram in figure 6 is a scatter plot of the biomass of sardines as a function of the 5-yr averages of SDR's. The population estimates used in figure 6 represent the spawning biomass of adults 2 years old and older.

Our regression of the sardine SDR with the revised population estimates yields a lower zero crossing than that obtained by Soutar and Isaacs (1974). This slightly improves the definition of population sizes where zero scale counts occur. Their zero crossing (MT of biomass at zero observed flux of scales) is approximately 700,000 MT compared to approximately 400,000 MT in figure 6.

The regression of anchovy-scale data versus biomass estimates is presented in the lower plot of figure 6. This analysis is based on data tabulated from Smith (1972), and includes two more data points than used in Soutar and Isaacs' (1974) comparison; we have added averages from two 5-year periods based on estimates of only two years of surveys (1940–44) and of four years (1965–69). This is done to gain more degrees of freedom but also adds more scatter to the earlier regression. Another important difference between this recalibration and that given by Soutar and Isaacs (1974) for the anchovy is the dramatic reduction in annual biomass estimates (see Smith and Moser 1988) as a result of work by Lo (1985) and Methot and Lo (1987). The implication of this work is that the spawning biomass estimates derived by Smith (1972) are now considered to be approximately four times too large (Smith, pers. comm.). Therefore we have reduced these values accordingly to compute the regression of anchovy biomass against the SDR data shown in the lower plot of figure 6.

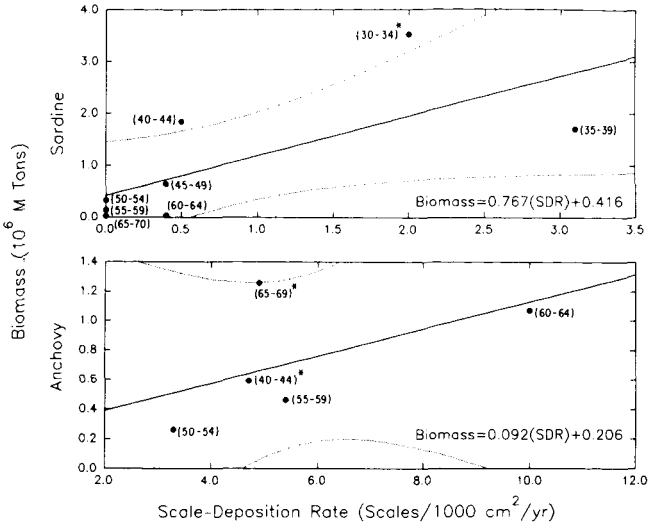

Figure 6. Linear regression of population biomass estimates of 2-yr-old and older Pacific sardine and northern anchovy (5-year averages) against the scale-deposition rates from the Santa Barbara Basin given by Soutar and Isaacs (1974). Sardine population estimates are from Murphy (1966; values from 1930 to 1944) and MacCall (1979; from 1945 to 1964). Anchovy population estimates are for the same years as in Soutar and Isaacs (1974) but with values strongly revised downwards (see Smith and Moser 1988). *Curved lines* show the 95% confidence interval around the regression line. Parenthetical numbers at data points refer to years of that pentad; the pentads marked by asterisks indicate population estimates based on less than 5-year averages for that pentad.

Using the regression equations shown in figure 6, we have transformed the SDR values of sardines and anchovies of figure 4 into units of biomass in figure 7. The regression of biomass against SDR values accounts for approximately 50% of the variance in the biomass of the sardine population and 31% of the variance in the anchovy population. The envelopes around the regression line in the scatter plots of figure 6 indicate the region in which 95% of the hindcast values are expected to fall.

The sardine hindcasts estimate the biomass between Punta Baja in Baja California and a point near Monterey, California (based on the area surveyed for the estimates obtained by MacCall [1979]). This corresponds to the "northern" sardine stock defined by Radovich (1981). The hindcasts of anchovy population are based on the estimates (Smith 1972) that include both the "central" and "southern" stocks of northern anchovy as defined by Vrooman et al. (1981). Thus the anchovy hindcasts in figure 7 refer to the adult biomass inhabiting inshore and offshore areas between roughly San Francisco, California, and Cabo San Lucas, Baja California.

TIME SCALES OF VARIABILITY IN THE SDR SERIES

Despite uncertainties in the varve chronology and the SDR estimates of population biomass, these records are valuable tools for exploring the variability occurring over time scales of several decades through several centuries. Figure 8 shows the variance spectra for the sardine and anchovy data after removal of long-term linear trends over the full length of both series. The spectral estimates have been smoothed by filtering with a cubic spline fit. The original sample resolution of 10-year intervals does not permit us to consider periods shorter than 20 to 30 years; to be completely safe we focus only on periods longer than 50 years.

In describing the time scales of variability, we distinguish between low-frequency variability and high-frequency variability based on the spectral characteristics of both the sardine and anchovy SDR

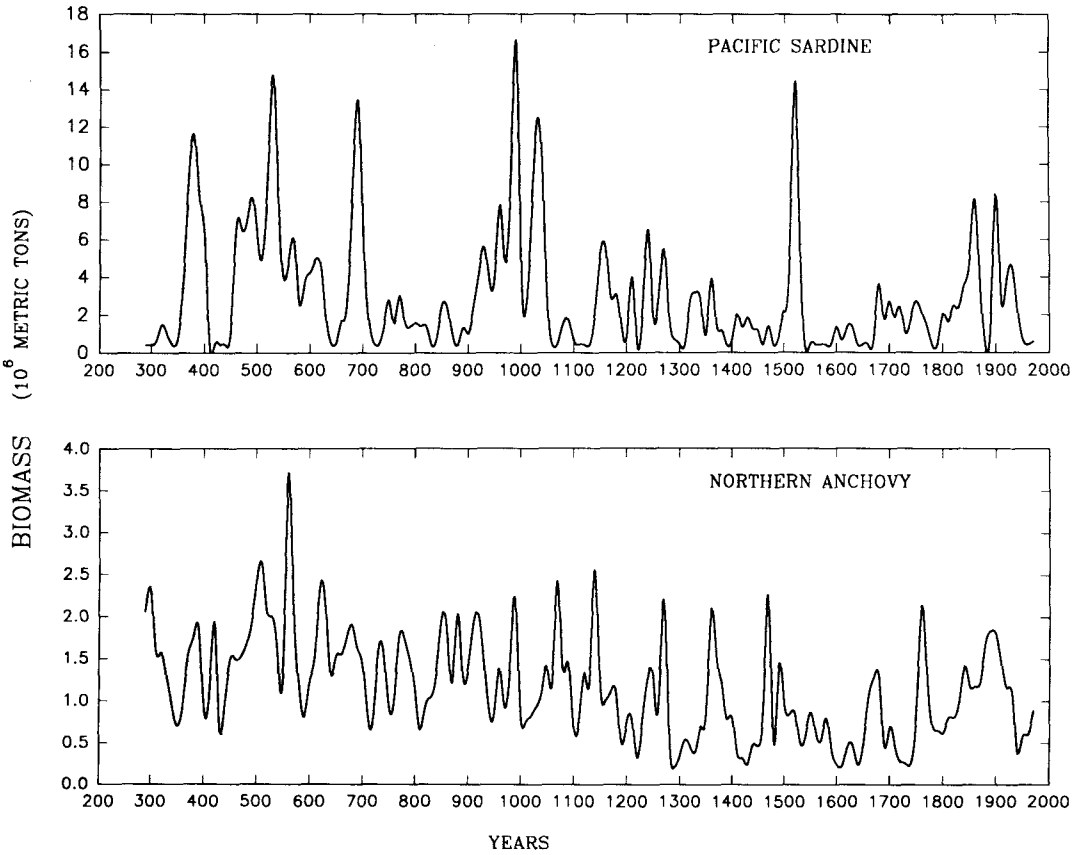

Figure 7. 1700-year hindcast series of Pacific sardine and northern anchovy biomasses off California and Baja California obtained by conversion of SDR data in figure 4 to units of biomass with the regression equations in figure 6.

series. For convenience we use the period of 150 years as a naturally occurring boundary between the high and low frequencies.

One noteworthy difference between spectra of the sardine and anchovy SDR data is the considerable variance centered around the 480- and 160-year periods in the sardine series. This appears to reflect low-frequency clumping in the sardine record, which does not appear in the anchovy record.

At the higher frequencies (periods shorter than 150 years), both the sardine and anchovy show peaks at nearly the same positions but with different levels of relative importance (near 60 years, between 70 and 80 years, and between 100 and 110 years). The 102-year peak dominates the spectrum of the anchovy data (figure 8); this reflects the strong regular organization of maximum and minimum values in the anchovy data of figure 4. In comparison, the 106-year peak in the sardine series is very weak. (The one-year precision in the position of spectral peaks is an artifact of calculation, since the sample resolution is only 10 years; thus peaks at 102 and 72 years should be rounded to 100 and 70 years, for example.)

We have separated the low-frequency variability (periods > 150 years) from the original sardine and anchovy series using a low-pass Spencer's 21-term filter (Statistical Graphics Corp. 1989) to produce the smooth curves through the original data points plotted in figure 9. Subtracting the deviations of the original from the filtered data gives us the time series of "residuals" plotted in figure 10. These are the extracted high-frequency components of the variance from the sardine and anchovy SDR series of figure 4, emphasizing periods in the range of 50 to 100 years. The spectra of the residual series (figure 11) allow us to view the relative importance of the shorter periods without interference from the low-frequency components.

The 57-year peak is more strongly emphasized (with respect to the other dominant peaks) in both the sardine and anchovy spectra of figure 11 than in figure 8. Figure 11 also clearly shows that the approximate 100-year peak for the anchovies is not present in the sardine data. The importance of the 100-year peak in the anchovy spectra of figure 11 is also diminished compared to its expression in figure

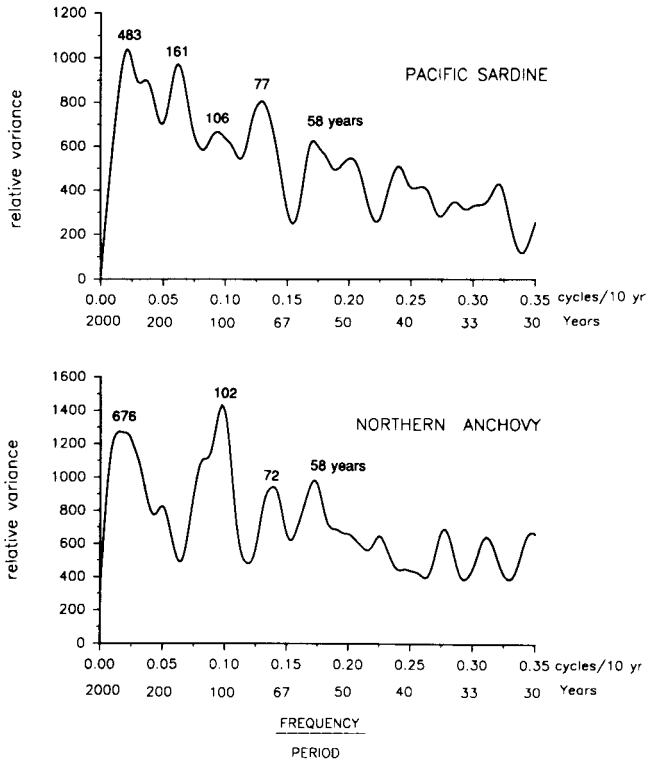

Figure 8. Smoothed power spectra of the scale-deposition rates of the Pacific sardine (*top*) and northern anchovy (*bottom*) that are plotted as time series in figure 4. Concentration of variance in specific frequency bands is identified with the corresponding time period, at the center of the spectral peaks.

8, reflecting a contribution of low-frequency variability to this peak in figure 8. We also see that both the importance and the offset between the 76-year (sardine) and 72-year (anchovy) peaks is maintained in figure 11.

Finally, it is important to point out that the correlation between the sardine and anchovy residuals of figure 10 ($R = 0.20$) is markedly lower than that for the original unfiltered series ($R = 0.33$) of figure 4, and much less than for the smoothed low-frequency data of figure 9 (which is $R = 0.56$). This important distinction has not been made in previous discussions of scale-deposition rates (e.g., Soutar and Isaacs 1974; Lasker and MacCall 1983; or Rothschild 1986). All these authors have remarked on the positive correlation, albeit weak, between the sardine and anchovy series. This positive correlation appears to be a response to the low-frequency components, and is negligible for periods less than 150 years. Cross-correlation of the two residual series of figure 10 also shows that there is no clear lag structure between the high-frequency components of the sardine and anchovy series (i.e., correlation is greatest at zero lag). Therefore the correlation is not simply reduced because of a consistent phase shift between the residual series.

RECOVERIES AND COLLAPSES OF THE PACIFIC SARDINE

The nature of fluctuations in the Pacific sardine population is particularly interesting as a background for better understanding the current recovery. The long records of sardine and anchovy SDR's allow us to examine the rise and fall of these populations as a series of collapses and recoveries. We can create a more visually concise record of the history of major declines and recoveries of the Pacific sardine by reducing the magnitudes of the sardine SDR values of figure 4 into four selected ranges: 0 scale deposition; ≤ 1 scale/10^3 cm^2 yr^{-1}; 1–5 scales/10^3 cm^2 yr^{-1}; and ≥ 5 scales/10^3 cm^2 yr^{-1}. The bottom plot of figure 12 is the simplified time series that corresponds to the new succession of clipped values obtained by expressing the data with these four categories. The estimated levels of biomass corresponding to these categories are given below the plot.

To establish a basis for examining population recoveries and declines, we define recovery and collapse in ways compatible with the record of scale deposition, and useful as a guide to past population behavior. We thus define recovery as a population expansion starting from less than or equal to approximately one million MT (from ≤ 1 SDR unit $\approx 1.2 \times 10^6$ MT) and climbing to a level equal to or greater than approximately four million MT (to ≥ 5 SDR units $\approx 4.2 \times 10^6$ MT). We chose a target biomass of four million MT or greater to represent a major recovery because that is the total biomass thought to have been present in the northern and southern subpopulations during the mid-1930s, when the fishery was at its peak of production (although the maximum biomass present before 1930 was considerably higher; Smith 1978). This level of biomass is also conveniently approximated by an SDR value of ≥ 5 units. The level of biomass chosen to represent the initial value at the beginning of a recovery (between near zero and roughly one million MT; approximated by the SDR values of ≥ 0 units and ≤ 1 unit) encompasses a very large range, but the sensitivity of the SDR values to low biomass values does not presently allow for greater precision. Collapses are defined as sustained population decreases from biomass levels starting above roughly four million MT and falling to one million MT or less.

Based on our definitions above, we recognize nine major recoveries and nine subsequent collapses of the sardine population off California in the past 1700 years. Eight recoveries begin from 0 SDR values (equivalent to $\leq 400{,}000$ MT), with one recovery

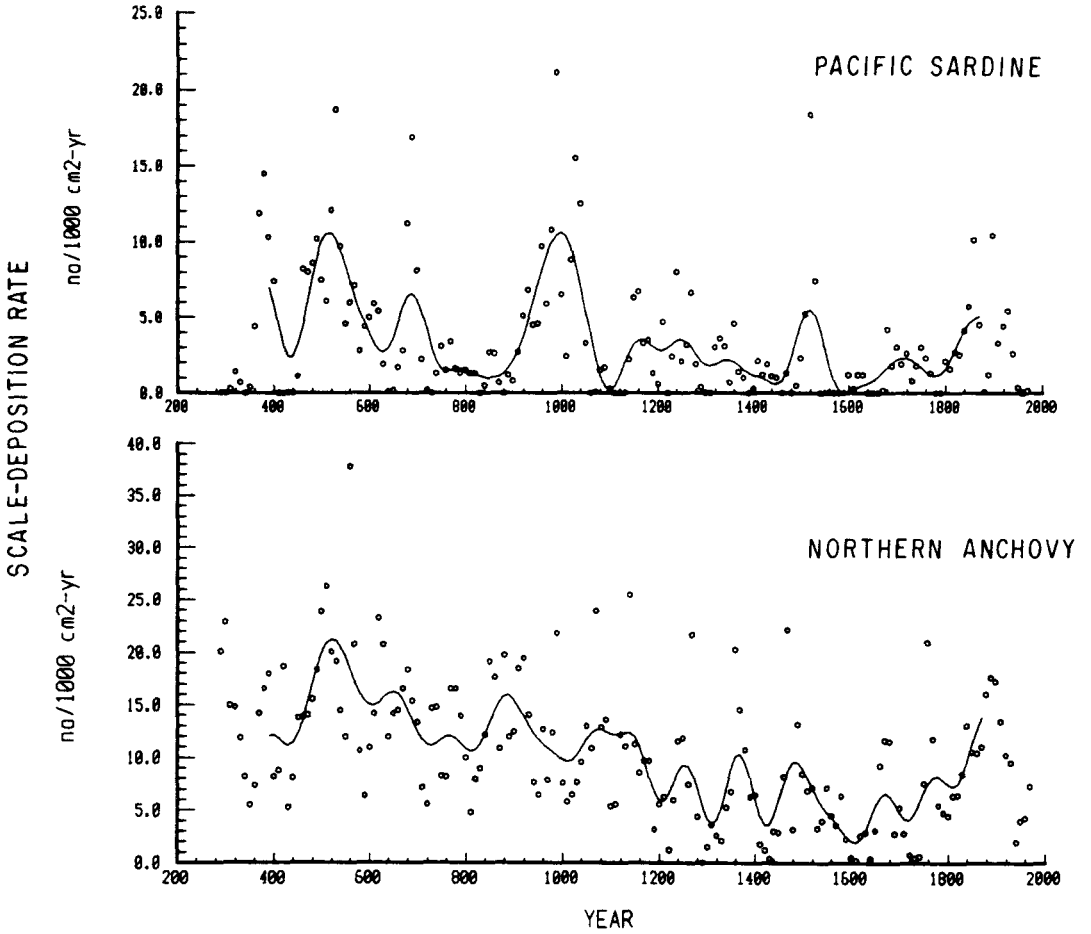

Figure 9. Extraction of the low-frequency variability (*continuous lines*) from the original data points (*circles*) of the Pacific sardine and northern anchovy SDR plots in figure 4. The continuous lines were obtained by low-pass filtering (using a 21-term Spencer filter); this effectively removes all periods longer than approximately 150 years from the original data (see figures 10 and 11).

starting from an initial value of $\leq 1.2 \times 10^6$ MT (≤ 1 SDR unit). Each interval of recovery and collapse is plotted in the upper part of figure 12.

The length of a recovery or decline is measured in decades because this is the smallest unit of time associated with our fish-scale chronology. We include as the initial decade of a recovery, for example, the first decade with a value of ≤ 1 SDR unit succeeding a decade of 0 SDR value; the final decade of the recovery is the first one in which a value of ≥ 5 SDR units occurs. Measured in this way (the temporal resolution is one decade) the recoveries range in length from 20 through 70 years, with an average duration of 36 years. The collapses range from 20 through 50 years, and average 30 years. Only two of the recovery events lasted for over 30 years; the longest of these lasted about 140 years. The upper plot in figure 12 indicates that most recoveries were followed relatively soon by collapses. Figure 12 also allows us to roughly compare the rate of the fishery-impacted decline during the 1940s with the average rate of declines through the past.

The rapid expansions of population size during the nine recoveries in figure 12 suggest that we can characterize an average recovery using the equation for simple exponential growth (neglecting, for now, the effects of density-dependence upon growth). Assuming a nominal prerecovery biomass of 10,000 MT and unrestrained exponential growth for the averaged 36-year period of a recovery, we determine a rate of population increase by substituting the average length of recovery (t = 36 years) and the post-recovery biomass ($N_{35} = 4.2 \times 10^6$ MT) into the equation

$$N_t = N_0 e^{rt}.$$

The rate of population growth for this period is then found to be $r = 0.17$ yr^{-1}, or approximately 17% per year. At t = 15 years after initiation of the recovery,

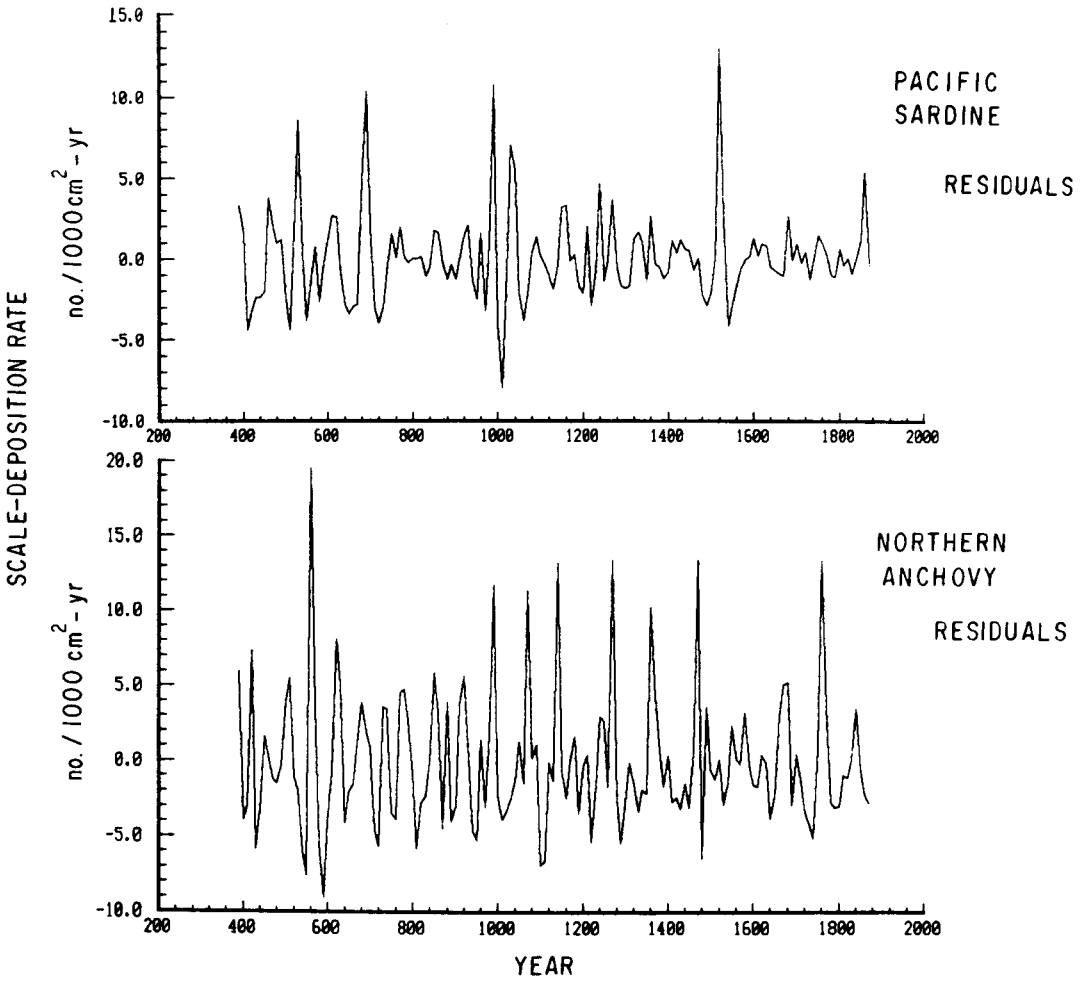

Figure 10. High-frequency components of variability in the Pacific sardine and northern anchovy SDR time series from figure 4. These values are the deviations (residuals) of the original data points from the smoothing function plotted in figure 9. Subtracting the original data from the filtered series leaves the high-frequency residuals containing variance with periods shorter than 150 years (see figure 11).

with this rate of increase, the population biomass would have grown to N_{15} = 128,070 MT.

We can test whether or not the characteristics of recoveries reconstructed from the scale-deposition rates are reasonable by comparing the above results to estimates for the present recovery of the Pacific sardine. Information presented by Barnes et al. (1992) indicates that the current recovery has been under way since the late 1970s—i.e., for approximately 15 years. The 1990 spawning biomass is estimated between 100,000 and 400,000 MT, and the rate of population increase since the early 1980s at around 30% per year. These figures are somewhat higher than we have obtained using the average-length recovery of 36 years as a guide. But they are very similar to the results we obtain by assuming a shorter recovery time of 25 years, which lies within the range observed for the nine recoveries described in figure 12.

Changing the recovery period to 25 years with the same initial and final biomass levels (10×10^3 and 4.2×10^6 MT) yields a growth rate of 24% per year. The biomass at 1990 (t = 13 years), predicted from the exponential growth equation, is then N_{13} = 231,224 MT. This exercise suggests that the current recovery of the Pacific sardine is occurring somewhat faster than an average, or canonical, recovery, but falls comfortably within the range of values for recoveries that can be derived from the SDR data.

DISCUSSION AND CONCLUSIONS

Although the Pacific sardine and northern anchovy have supported major fisheries off California during the twentieth century, volatility in these stocks has made them notoriously difficult to manage. Their boom-and-bust history has been attributed, in varying degrees, to overintensive fishing,

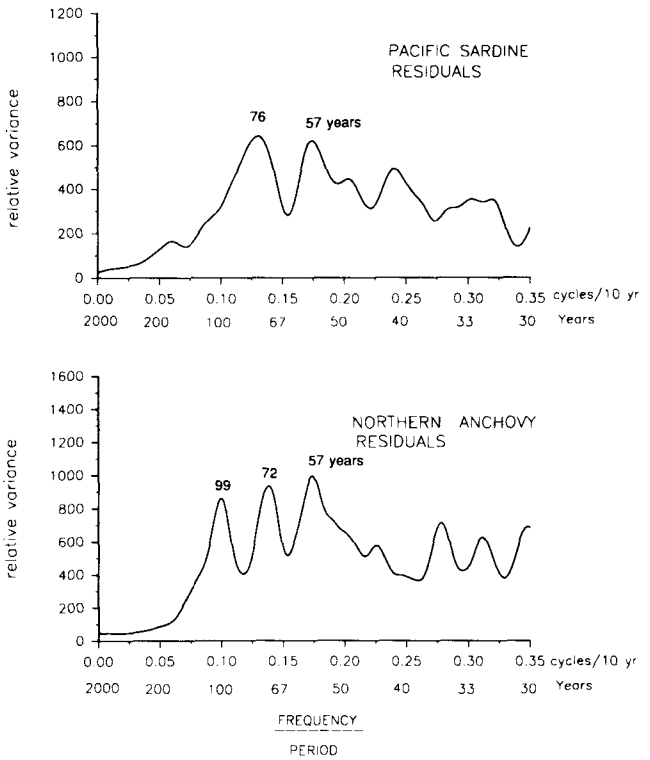

Figure 11. Power spectra of the isolated high-frequency components (residuals) of the Pacific sardine and northern anchovy SDR time series from figure 10. Major spectral peaks are identified with the corresponding time period. Note the abrupt cutoff of variance at periods longer than approximately 150 to 200 years.

biological interaction within and among species, and environmental controls associated with large-scale climatic change. The perspective provided by our improved 1700-year reconstruction of scale-deposition rates in figure 4 should provide critical insights needed to unravel the sources of variability in these fish stocks.

We caution, however, that these data are still based on a relatively small area of depositional surface with respect to the density of scales (particularly those of the sardine) found in the sediment. The area of the two piston cores (214 and 224) constitutes roughly 10% of that of the four box cores (see figure 5) used for the uppermost section (Soutar and Isaacs 1974). Our analysis of the signal-to-noise ratios indicates a need for further sampling of the long time series to capture the complete range of variability of SDR's over the basin. This means recovering the upper 2–3 m of sediment with devices such as box-type Kasten corers, which sample an effective area of 100 cm^2 or greater. This is particularly important to permit replicate sampling of multiple cores to distinguish possible "interaction" between spatial and temporal variability in SDR values over the basin.

In addition to a clean and verifiable signal in the SDR's, chronological accuracy is the other crucial ingredient for reconstructing the series of SDR values in figure 4. Although we believe the chronology

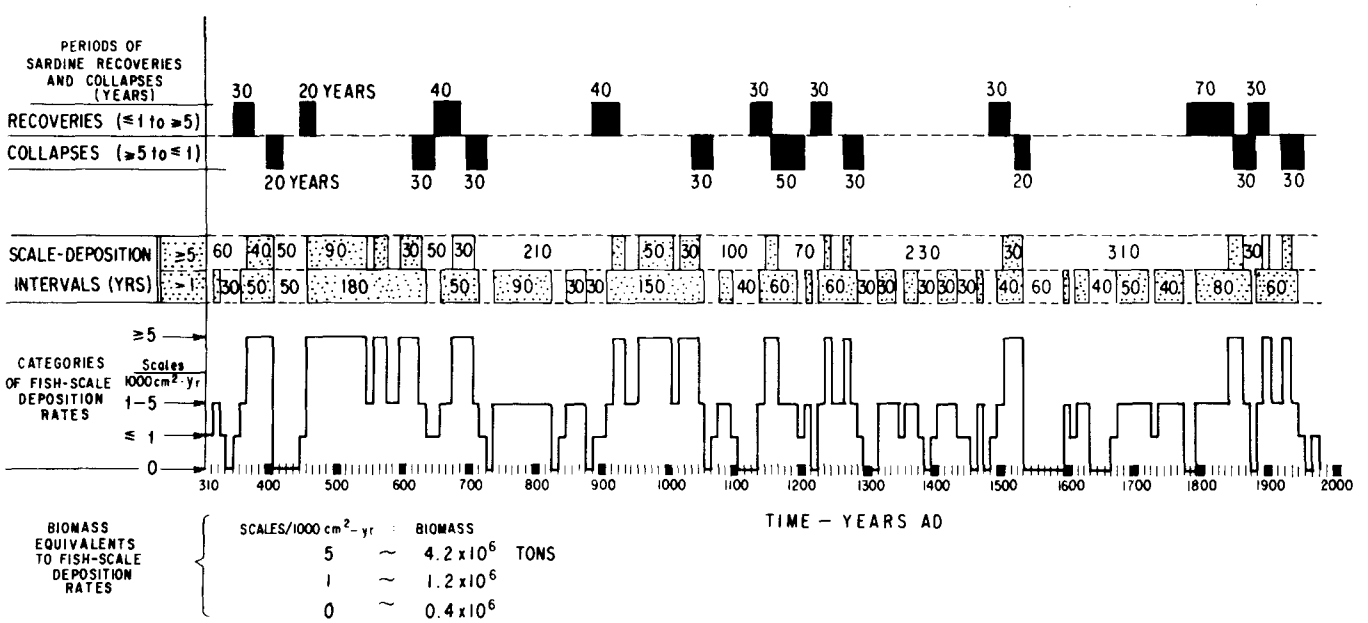

Figure 12. Pacific sardine SDR data from figure 4 plotted according to four selected ranges of values. The continuously varying curve of figure 4 has been transformed into a step function (*lower plot*), which takes on the values of 0 scale deposition; ≤1 scale/10^3 cm^2 yr^{-1}; 1–5 scales/10^3 cm^2 yr^{-1}; or ≥5 scales/10^3 cm^2 yr^{-1}. Biomass levels equivalent to these SDR values are listed at the bottom of the lower plot. The nine periods of recoveries and collapses of the sardine population inferred from the SDR time series are plotted above as darkened blocks corresponding to increases from ≤1 to ≥5 SDR units and declines from ≥5 SDR to ≤1 SDR units.

supporting figure 4 is a substantial improvement from figures 2 and 3, another similar adjustment may still prove necessary. Ultimately the desired accuracy necessary to solidly anchor the varve chronology to calendar time must be sought through independent, detailed radiometric dating. This has not been pursued so far because of the poor precision of available radiometric techniques applied to ocean sediments less than 2000 years old. However, we are now involved in an effort to provide an independent radiocarbon chronology using high-precision AMS techniques on sources of terrestrial carbon in the varved sediments.

The relationship between the SDR data and modern population estimates (figure 6) gives us a means to hindcast the estimates of population biomasses over the past 1700 years (figure 7). The accuracy of this hindcast is, however, limited not only by chronological uncertainty but also by the uncertainty evident in calibration of the SDR values. An important goal of future work will be to upgrade this calibration by appending data from recent decades (during which the population sizes of sardines and anchovies have changed substantially) to the data of figure 6 through further box coring.

Development of the long time series of SDR's in figure 4 has enabled us to begin an exploratory analysis of the decadal-through-centennial time scales of variability in the sardine and anchovy populations. To begin, we have separated the variance of the fish-scale series into its higher-frequency versus lower-frequency components using a period of about 150 years as a convenient natural boundary. In the high-frequency part of the spectra, both anchovies and sardines fluctuate at a period of approximately 60 years. Conversely, a 100-year period is very important in the anchovy data, but is completely missing in the sardine spectrum. At lower frequencies the anchovies appear to fluctuate with a longer period (680 years) than do the sardines (480 years).

We find that the weak positive correlation between the sardine and anchovy series (noted by Soutar and Isaacs [1974] for the period of 1810–1970) is carried by the low-frequency component of the variances (periods of 150 years and longer; cf. figures 9 and 10). This is an important observation, since the weak positive correlation between these two species has been used to question Murphy's (1966) suggestion that replacement of the sardines by anchovies in the California Current implied a competition for food resources (Radovich 1981).

Lasker and MacCall (1983) suggested that the weak correlation signified a parallel response to large-scale environmental change. Their explanation seems quite reasonable for very-long-period change, but perhaps not so much for periods less than 150 years. For example, the lack of any lagged cross-correlation of the high-frequency variability of sardines and anchovies indicates that there is no consistent phase shift associated with the 60-year period exhibited by both species. This appears to be as consistent with a hypothesis for competition or some other biological interaction as with a hypothesis for mediation through environmental change. We are presently using our analysis of the time scales of variability to search for evidence or suggestions of the sources of the variability.

Lumping all the sardine SDR data into four categories of increasing magnitude (figure 12) provides a simplified version of the population's overall variability through time. We perceive a tendency toward two alternating long-lived regimes of SDR's due to the general clustering of the high values ($\geq$5 SDR units; encompassing over 25% of the record) and a persistence of the intermediate values (1–5 SDR units; 41% of the record). These two long-term regimes (200 years and greater) are interrupted by short-term or abrupt dips in the SDR values, which occur over periods of approximately 30–40 years, reflecting the 60–80-year periods shown in figures 8 and 11. The general persistence and abrupt shifts in biomass levels in figure 12 may reflect two alternating states in habitat suitability during the last 2000 years.

Finally, our analysis of the history of scale deposition in the Santa Barbara Basin provides a useful perspective on the current recovery of the Pacific sardine. We find that this recovery is not unlike those of the past in its rate, magnitude, and overall evolution (figure 12). Neither was the sardine collapse that began in the 1940s unlike earlier collapses. This does not necessarily mean, however, that the current cycle of collapse and recovery has no relation to the application/release of fishing pressure, or change in ocean climate, or both. What we infer is (as well as we can determine from the resolution of a 10-year sampling window) that the rates and magnitudes of the recoveries and the collapses can generally be described by relatively few parameters. This suggests that even though the causes, and perhaps the mechanisms, may vary for different recoveries or collapses, the sustained reproductive consequences (success for recoveries and failure for collapses) are similar from one event to another.

ACKNOWLEDGMENTS

This paper is funded in part by a grant from the National Sea Grant College Program, National

Oceanic and Atmospheric Administration, U.S. Department of Commerce, under grant number NOAA NA89AA-D-SG138 1991–92, project number 48-F-N through the California Sea Grant College, and in part by the California State Resources Agency. The views expressed herein are those of the authors and do not necessarily reflect the views of NOAA or any of its subagencies. The U.S. government is authorized to reproduce and distribute for governmental purposes. We also acknowledge the generous support received both from the Centro de Investigación Científica y Educación Superior de Ensenada through block funding from the government of Mexico, and from the Marine Life Research Group of the Scripps Institution of Oceanography. We thank Michael Mullin, Elizabeth Venrick, and two anonymous reviewers for valuable criticism to improve the final manuscript.

LITERATURE CITED

Barnes, J. T., L. D. Jacobson, A. D. MacCall, and P. Wolf. 1992. Recent population trends and abundance estimates for the Pacific sardine (*Sardinops sagax*). Calif. Coop. Oceanic Fish. Invest. Rep. 33 (this volume).

Bruland, K. W., R. P. Franks, W. M. Landing, and A. Soutar. 1981. Southern California inner basin sediment trap calibration. Earth and Planetary Sci. Lett. 53:400–408.

Byrne, R., J. Michaelsen, and A. Soutar. In press. Prehistoric wildfire frequencies in the Los Padres National Forest: fossil charcoal evidence from the Santa Barbara Channel. U.S. Forest Service Tech. Rep., 78 pp.

DeVries, T. J., and W. G. Pearcy. 1982. Fish debris in sediments of the upwelling zone off central Peru: a late Quaternary record. Deep Sea Res. 28:87–109.

Enfield, D. B., and J. S. Allen. 1980. On the structure and dynamics of monthly mean sea level anomalies along the Pacific coast of North and South America. J. Phys. Oceanogr. 10:557–578.

Fleischer, P. 1972. Mineralogy and sedimentation history, Santa Barbara Basin, California. Sediment. Petrol. 42:49–58.

Griffiths, J. C. 1967. Scientific method in the analysis of sediments. New York: McGraw-Hill, 508 pp.

Heusser, L. 1978. Pollen in Santa Barbara Basin, California: a 12,000-yr record. Geol. Soc. Am. Bull. 89:673–678.

Koide, M., A. Soutar, and E. D. Goldberg. 1972. Marine geochronology with ^{210}Pb. Earth and Planetary Sci. Lett. 14:442–446.

LaMarche, V. C. 1974. Paleoclimatic inferences from long tree-ring records. Science 183:1043–1048.

Lasker, R., and A. MacCall. 1983. New ideas on the fluctuations of clupeoid stocks off California, *In* Proceedings of the Joint Oceanographic Assembly 1982—general symposia. Canadian National Committee/Scientific Committee on Oceanic Research. Ottawa, Ont., pp. 110–120.

Lo, N. C. H. 1985. Egg production of the central stock of northern anchovy, *Engraulis mordax*, 1951–1982. Fish. Bull., U.S. 83:137–150.

MacCall, A. D. 1979. Population estimates for the waning years of the Pacific sardine fishery. Calif. Coop. Oceanic Fish. Invest. Rep. 20: 72–82.

Methot, R. D., and N. C. H. Lo. 1987. Spawning biomass of the northern anchovy in 1987. SWFC Admin. Rep., La Jolla, LJ-87-14.

Murphy, G. I. 1966. Population biology of the Pacific sardine (*Sardinops caerulea*). Proc. Calif. Acad. Sci. 34:1–84.

Pisias, N. G. 1978. Paleoceanography of the Santa Barbara Basin during the last 8000 years. Quat. Res. 10:366–384.

Radovich, J. 1981. The collapse of the California sardine fishery—what have we learned? *In* Resource management and environmental uncertainty, M. H. Glantz and J. D. Thompson, eds. Wiley series in advances in environmental science and technology, vol. 11. New York: Wiley-Interscience, pp. 107–136.

Rothschild, B. J. 1986. Dynamics of marine fish populations. Cambridge, Mass: Harvard Univ. Press, 277 pp.

Schimmelmann, A., K. Lange, J. Michaelsen, and W. Berger. 1990. Climatic changes reflected in laminated Santa Barbara Basin sediments. *In* Proceedings of the sixth annual Pacific Climate (PACLIM) workshop, J. L. Betancourt and A. M. MacKay, eds. California Department of Water Resources, Interagency Ecological Studies Program Tech. Rep. 23, Sacramento. Pp. 97–99.

Shackleton, L. Y. 1986. An assessment of the reliability of fossil pilchard and anchovy scales as fish population indicators off Namibia. M.Sc. thesis, Univ. Cape Town, South Africa, 141 pp.

Sholkovitz, E. R. 1973. Interstitial water chemistry of the Santa Barbara Basin sediments. Geochim. Cosmochim. Acta 37:2043–2073.

Smith, P. E. 1972. The increase in spawning biomass of northern anchovy, *Engraulis mordax*. Fish. Bull., U.S. 70:849–874.

———. 1978. Biological effects of ocean variability: time and space scales of biological response. Rapp. P.-V. Réun. Cons. Int. Explor. Mer 173:117–127.

Smith, P. E., and H. G. Moser. 1988. CalCOFI time series: an overview of fishes. Calif. Coop. Oceanic Fish. Invest. Rep. 29:66–77.

Soutar, A. 1967. The accumulation of fish debris in certain California coastal sediments. Calif. Coop. Oceanic Fish. Invest. Rep. 11:136–139.

Soutar, A., and P. A. Crill. 1977. Sedimentation and climatic patterns in the Santa Barbara Basin during the 19th and 20th centuries. Geol. Soc. Am. Bull. 88:1161–1172.

Soutar A., and J. D. Isaacs. 1969. History of fish populations inferred from fish scales in anaerobic sediments off California. Calif. Coop. Oceanic Fish. Invest. Rep. 13:63–70.

———. 1974. Abundance of pelagic fish during the 19th and 20th centuries as recorded in anaerobic sediment of the Californias. Fish. Bull. 72:257–273.

Statistical Graphics Corp. 1989. Statgraphics: a statistical-graphics system.

Suess, E. 1981. Phosphate regeneration from sediments of the Peru continental margin by dissolution of fish debris. Geochim. Cosmochim. Acta 45:577–588.

Vrooman, A. M., P. A. Paloma, and J. R. Zweifel. 1981. Electrophoretic, morphometric and meristic studies of subpopulations of northern anchovy, *Engraulis mordax*. Calif. Fish Game 67(1):39–51.